

Thermodynamics of Pyridine Coordination in 1,4-Phenylene Bridged Bimetallic (Pd, Pt) Complexes Containing Two *N,C,N'* Motifs, 1,4- M_2 -[$C_6(CH_2NR_2)_{4-2,3,5,6}$]

Sung Lan Jeon, David M. Loveless, Wayne C. Yount, and Stephen L. Craig*

Department of Chemistry and Center for Biologically Inspired Materials and Material Systems, Duke University, Durham, North Carolina 27708-0346

Received June 29, 2006

The thermodynamics of pyridine coordination in 1,4-phenylene-bridged binuclear palladium and platinum organometallic complexes [1,4-(MOTf)₂-{C₆(CH₂NR₂)_{4-2,3,5,6}}] (**11**, M = Pd, Pt; R = CH₃, C₂H₅, R₂ = -(CH₂)₅-) are measured by ¹H NMR in DMSO-*d*₆. The coordination of substituted pyridines by bimetallic complexes **11** or **12** in DMSO is found to proceed via two effectively independent metalligand binding events, and the association constants for pyridine coordination and rate constants for pyridine exchange are nearly identical to those measured previously on monometallic analogs. A linear free energy relationship between the association constant for pyridine coordination and the inductive Hammett constant of the pyridine substituent is observed, and the sensitivity ($\rho = -1.7$ to -2.1) in DMSO depends only slightly on metal (Pd vs Pt) and spectator ligand (pincer dialkylamine vs triarylphosphine). The association constant for a particular pyridine ligand, however, varies by roughly 3 orders of magnitude across the series of metal complexes. The effective independence of the two coordination sites and the range of available thermodynamic and kinetic behaviors of the coordination guide the use of these versatile building blocks in metallosupramolecular applications.

Background and Introduction

Pincer-type organometallic complexes are excellent functional units in macroscopic applications, e.g., in catalysis,¹ the stabilization of unstable cationic complexes,² sensing,³ molecular switches,^{4–5} and the preparation of organometallic supramolecular structures and materials.^{6–10} Among the more

commonly used ligands within the bifunctional pincer-type organometallic complexes are the *N,C,N'*-terdentate coordinating aryl ligands [C₆H₂-2,6-(CH₂NMe₂)₂][–] (NCN)^{11–13} and related bis(pincer) ligands such as the 1,4-phenylene-bridged

* To whom correspondence should be addressed. E-mail: stephen.craig@duke.edu.

- (1) (a) Halpern, J. *Pure Appl. Chem.* **2001**, *73*, 209–220. (b) Loch, J. A.; Crabtree, R. H. *Pure Appl. Chem.* **2001**, *73*, 119–128. (c) Morales-Morales, D.; Redon, R.; Yung, C.; Jensen, C. M. *Inorg. Chim. Acta* **2004**, *357*, 2953–2956. (d) Naghipour, A.; Sabounchei, S. J.; Morales-Morales, D.; Hernandez-Ortega, S.; Jensen, C. M. *J. Organomet. Chem.* **2004**, *689*, 2494–2502. (e) Dijkstra, H. P.; Slagt, M. Q.; McDonal, A.; Kruithof, C. A.; Kreiter, R.; Mills, A. M.; Lutz, M.; Spek, A. L.; Klopper, W.; van Klink, G. P. M.; van Koten, G. *Eur. J. Inorg. Chem.* **2003**, 830–838.
- (2) Gandelman, M.; Konstantinovski, L.; Rozenberg, H.; Milstein, D. *Chem. Eur. J.* **2003**, *9*, 2595. (b) Poverenov, E.; Leitius, G.; Shimon, L. J. W.; Milstein, D. *Organometallics* **2005**, *24*, 5937–5944.
- (3) (a) Albrecht, M.; Schlupp, M.; Bargon, J.; van Koten, G. *Chem. Commun.* **2001**, 1874–1875. (b) Seward, C.; Jia, W.-L.; Wang, R. Y.; Wang, S. *Inorg. Chem.* **2004**, *43*, 978–985.
- (4) Albrecht, M.; Lutz, M.; Spek, A. L.; van Koten, G. *Nature* **2000**, *406*, 970–974.
- (5) Steenwinkel, P.; Grove, D. M.; Veldman, N.; Spek, A. L.; van Koten, G. *Organometallics* **1998**, *17*, 5647–5655.

- (6) Steenwinkel, P.; Kooijman, H.; Smeets, W. J. J.; Spek, A. L.; Grove, D. M.; van Koten, G. *Organometallics* **1998**, *17*, 5411–5426.
- (7) (a) Alsters, P. L.; Baesjou, P. J.; Janssen, M. D.; Kooijman, H.; Sicherer-Roetman, A.; Spek, A. L.; van Koten, G. *Organometallics* **1992**, *11*, 4124–4135. (b) Rodriguez, G.; Albrecht, M.; Schoenmaker, J.; Ford, A.; Lutz, M.; Spek, A. L.; van Koten, G. *J. Am. Chem. Soc.* **2002**, *124*, 5127–5138. (c) Amijs, C. H. M.; Berger, A.; Soulimani, F.; Visser, T.; van Klink, G. P. M.; Lutz, M.; Spek, A. L.; van Koten, G. *Inorg. Chem.* **2005**, *44*, 6567–6578.
- (8) Albrecht, M.; van Koten, G. *Angew. Chem., Int. Ed.* **2001**, *40*, 3750–3781.
- (9) Huck, W. T. S.; Prins, L. J.; Fokkens, R. H.; Nibbering, N. M. N.; van Veggel, F. C. J. M.; Reinhoudt, D. N. *J. Am. Chem. Soc.* **1998**, *120*, 6240–6246.
- (10) (a) Pollino, J. M.; Weck, M. *Synthesis* **2002**, 1277–1285; Pollino, J. M.; Stubbs, L. P.; Weck, M. *J. Am. Chem. Soc.* **2004**, *126*, 563–567. (b) Pollino, J. M.; Weck, M. *Chem. Soc. Rev.* **2005**, *34*, 193–207.
- (11) Knapen, J. W. J.; van der Made, A. W.; de Wilde, J. C.; van Leeuwen, P. W. N. M.; Wijkens, P.; Grove, D. M.; van Koten, G. *Nature* **1994**, *372*, 659–663.
- (12) van de Kuil, L. A.; Luitjes, H.; Grove, D. M.; Zwikker, J. W.; van der Linden, J. G. M.; Roelofs, A. M.; Jenneskens, L. W.; Drenth, W.; van Koten, G. *Organometallics* **1994**, *13*, 468–477.
- (13) van de Kuil, L. A.; Grove, D. M.; Zwikker, J. W.; Jenneskens, L. W.; Drenth, W.; van Koten, G. *Chem. Mater.* **1994**, *6*, 1675–1683.

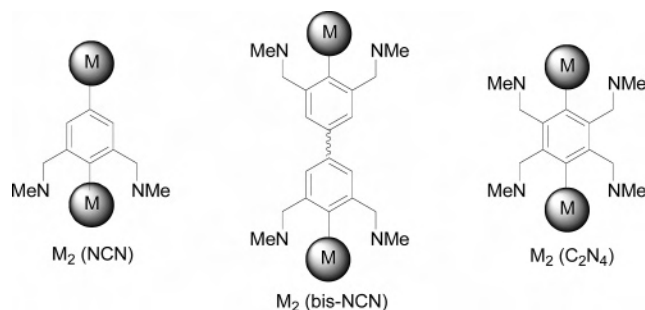


Figure 1. Schematic representation of the bifunctional pincer-type organometallic complexes containing one or two NCN motifs.

ligand $[\text{C}_6(\text{CH}_2\text{NR}_2)_4\text{-}2,3,5,6]^{2-}$ (C_2N_4)⁵ and the 4,4'-biphenylene bridged bis-NCN ligand (bis-NCN) (Figure 1).^{6,14–15} The synthesis and many functional properties of these pincer motifs have been studied extensively by van Koten^{5–8,11–17} and others.¹⁸

Our specific interest in these compounds arises from their use as mechanistic probes of the dynamic molecular processes underlying the mechanical properties of mainchain reversible polymers (RPs)¹⁹ and supramolecular networks.²⁰ We recently reported that steric effects in the alkylamine substituents of pincer Pd(II) and Pt(II) complexes allow for pseudo-independent control of ligand exchange kinetics relative to the thermodynamics of association vs competing DMSO coordination.¹⁹ The combined Pd and Pt series of compounds span dissociation timescales from milliseconds to tens of minutes, so that a wide range of dynamic materials behaviors might be addressed. In addition to the ease of steric manipulation within the spectator ligands, the pincer complexes have the added advantage of increased stability,²¹ a particularly attractive feature given the moderate stability of many aryl Pd(II) organometallic complexes. The pincer systems are also amenable to numerous structural modifications through the organometallic aryl group, metal, pincer ligands, counterion, and associating ligand. These modifications allow the motif to be tailored to numerous desired polymeric endpoints (e.g., solubility, variations in persistence length, and cohesive energy density).

The 1,4-phenylene-bridged complexes^{5,22d} contain the shortest possible aromatic spacer between pincer functionalities, and the motif therefore creates the minimal inherent structural perturbation to the remainder of a polymeric

platform. Furthermore, the rigidity and directionality of the linker ensure that the persistence length of RPs is not limited by the bimetallic component. The concise synthesis of bimetallic complexes **3** and **5**, reported previously by van Koten, established that their preparation could be realized on a gram scale (Scheme 1).^{5–6,14–15}

To take full advantage of the attractive characteristics of the 1,4-phenylene-bridged complexes in the study of bulk materials, the thermodynamics and kinetics of reversible ligand coordination, particularly those of pyridine derivatives, must be quantified. Although coordination complexes between substituted pyridines and Pd(II)- and Pt(II)-containing organometallic species have a considerable presence in a range of thermodynamically²² and kinetically^{23–24} controlled assembly processes, we are unaware of more than a few published thermodynamic data²² for these associations in pincer motifs. Most notably, van Manen et al. have reported a linear free energy relationship for the effect of pyridine substituent on complexation to SCS–Pd(II) pincer systems.^{22d}

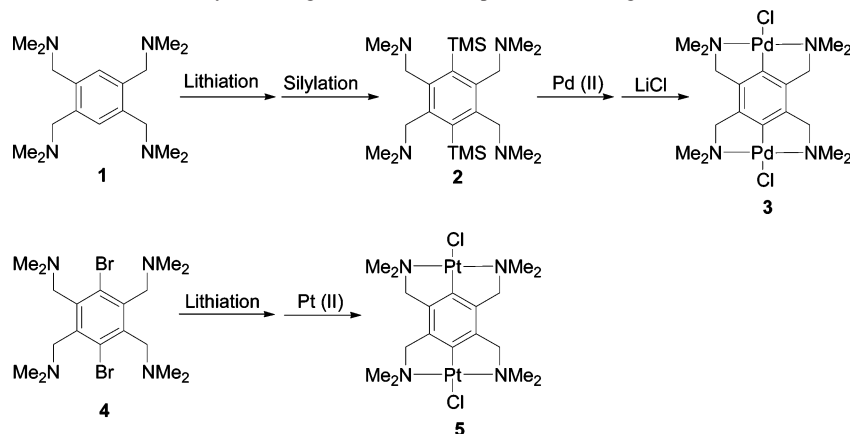
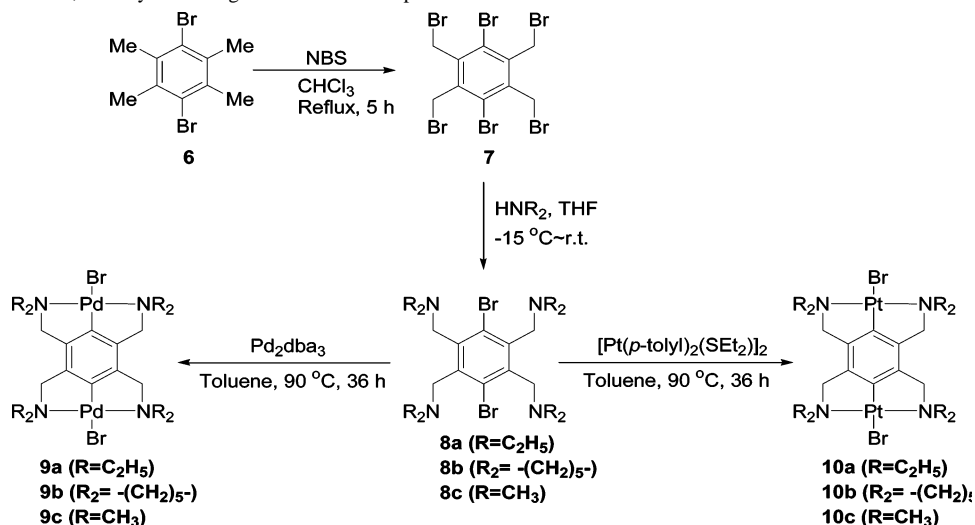
We report here the thermodynamics of metalpyridine coordination in DMSO to the metal coordination sites of 1,4-phenylene-bridged bimetallic (Pd, Pt) complexes. The relative independence of the two sites is demonstrated, as is the similarity in the thermodynamics and kinetics of coordination vs those of a monofunctional model system. The effect of the metal (Pd vs Pt) and spectator ligands (pincer NCN vs triarylphosphine) on the relative binding affinities of substituted pyridine ligands is examined and compared to complexation to SCS–Pd(II) pincer complexes reported previously by van Manen. Notably, the *relative* affinity of substituted pyridine ligands depends on the solvent. These studies extend the foundation underlying the use of these pincer complexes in a range of metallosupramolecular chemistries, including investigations of supramolecular polymer mechanics and mechanisms.

Results and Discussion

Synthesis and Characterization. The synthesis of 1,4-phenylene-bridged bimetallic complexes **9–10** proceeded through the appropriate 1,4-dibromo derivatives $[\text{C}_6\text{Br}_2(\text{CH}_2\text{NR}_2)_4\text{-}2,3,5,6]$ (**8**) (Scheme 2). The use of the 1,4-dibromo intermediates was necessitated by poor yields in the preparation of **1** and its octa(ethyl) congeners, prepared by the amination of 1,2,4,5-tetrakis(bromomethyl)benzene. While the amination with dimethylamine provided the desired tetrakis(dimethylamino) derivative **1** in 38% yield,¹⁴ the amination with diethylamine produced only a small, unisolable fraction of the desired compound within a multicom-

- (14) Steenwinkel, P.; Jastrzebski, J. T. B. H.; Deelman, B.-J.; Grove, D. M.; Kooijman, H.; Veldman, N.; Smeets, W. J. J.; Spek, A. L.; van Koten, G. *Organometallics* **1997**, *16*, 5486–5498.
- (15) Steenwinkel, P.; James, S. L.; Grove, D. M.; Kooijman, H.; Spek, A. L.; van Koten, G. *Organometallics* **1997**, *16*, 513–515.
- (16) Sutter, J.-P.; Grove, D. M.; Beley, M.; Collin, J.-P.; Veldman, N.; Spek, A. L.; Sauvage, J.-P.; van Koten, G. *Angew. Chem., Int. Ed.* **1994**, *33*, 1282–1285.
- (17) Lagunas, M.-C.; Gossage, R. A.; Spek, A. L.; van Koten, G. *Organometallics* **1998**, *17*, 731–741.
- (18) Loeb, S. J.; Shimizu, G. K. H. *J. Chem. Soc., Chem. Commun.* **1993**, 1395–1397.
- (19) Yount, W. C.; Juwarker, H.; Craig, S. L. *J. Am. Chem. Soc.* **2003**, *125*, 15302–15303.
- (20) (a) Yount, W. C.; Loveless, D. M.; Craig, S. L. *Angew. Chem., Int. Ed.* **2005**, *44*, 2746–2748. (b) Yount, W. C.; Loveless, D. M.; Craig, S. L. *J. Am. Chem. Soc.* **2005**, *127*, 14488–14496.
- (21) Slagt, M. Q.; Rodriguez, G.; Grutters, M. M. P.; Gebbink, R. J. M. K.; Klopper, W.; Jenneskens, L. W.; Lutz, M.; Spek, A. L.; van Koten, G. *Chem. Eur. J.* **2004**, *10*, 1331–1344.

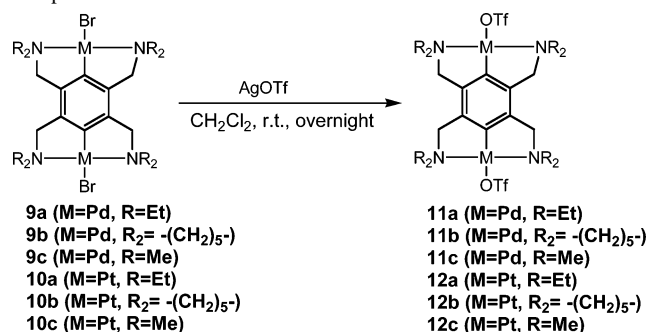
- (22) (a) Lowry, T. H.; Richardson, K. S. *Mechanism and Theory in Organic Chemistry, Harper International Edition*; Harper Collins Publishers: New York, 1987. (b) Ashcroft, S. J.; Mortimer, C. T. *Thermochemistry of Transition Metal Complexes*; Academic Press: London, New York, 1970. (c) Gerhardt, W. W.; Weck, M. *J. Org. Chem.* **2005**, submitted for publication. (d) van Manen, H.-J.; Nakashima, K.; Shinkai, S.; Kooijman, H.; Spek, A. L.; van Veggel, F. C. J. M.; Reinhoudt, D. N. *Eur. J. Inorg. Chem.* **2000**, 2533–2540.
- (23) Kurosawa, H.; Urabe, A.; Emoto, M. *J. Chem. Soc., Dalton Trans.* **1986**, 4, 891–893.
- (24) Rauth, G. K.; Mahapatra, A.; Sinha, C. *Inorg. React. Mech.* **2002**, 57–65.

Scheme 1. Previous Synthetic Route to 1,4-Phenylene-Bridged Bimetallic Complexes Containing C₂N₄**Scheme 2.** Synthesis of 1,4-Phenylene-Bridged Bimetallic Complexes 9–10

ponent mixture of products. Bromination of 1,4-dibromo-2,3,5,6-tetramethylbenzene (**6**)²⁵ to 1,4-Br₂-{C₆(CH₂Br)₄-2,3,5,6} (**7**)^{26a} (75% yield) followed a process previously used to make 1,2,4,5-tetrakis(bromomethyl)benzene.^{26b} Subsequent nucleophilic amination of **7** with HNR₂ (R = CH₃,¹⁴ C₂H₅, R₂ = -(CH₂)₅-) provided 1,4-Br₂[C₂N₄] (**8**) in greater yields (>91%) than obtained for the similar reaction of 1,2,4,5-tetrakis(bromomethyl)benzene.

Compounds **8** are directly reacted with Pd₂(dba)₃ or [Pt(*p*-tolyl)₂(SEt₂)₂]²⁷ in toluene for 36 h at 90 °C to afford 1,4-phenylene-bridged bipalladium complexes **9** or biplatinum complexes **10** in a manner similar to that reported for monometallic analogues⁷ (72–94%). Reaction of bimetallic compounds **9** or **10** with AgOTf yields the desired bistriflate complexes **11–12** in excellent yields (>94%) (Scheme 3). These labile, bistriflate complexes were then used in subsequent studies of the thermodynamics and kinetics of pyridine association and exchange.

The aryl 1,4-dibromo compounds **8** provide a potential intermediate for complementary lithiation routes to com-

Scheme 3. Synthesis of Bistriflated 1,4-Phenylene-Bridged Bimetallic Complexes **11** and **12**

pounds **10**, similar to the original van Koten synthesis (Scheme 1).⁶ For example, bis-Pt(II) compound **5**⁶ is obtained from the reaction of platinum(II) substrates such as [PtCl₂(SEt₂)₂]²⁸ with the lithium derivatives 1,4-Li₂[C₂N₄] that are generated from compound **8c** (same compound as **4**)¹⁴ and *n*-BuLi. In this approach, however, the tetrakis(diethylamino) platform again proved to be problematic. Lithiation and an attempted subsequent platination afforded not the desired bis-(platinum) compound **10a** but the debrominated analog of compound **8**. Apparently, the reaction of the lithiated

(25) Porwisiak, J.; Dmowski, W. *Synth. Commun.* **1989**, *19*, 3221–3229.(26) (a) Hopff, H.; Doswald, P.; Manukian, B. K. *Helv. Chim. Acta* **1961**, *44*, 1231–1237. (b) Wu, A.-T.; Liu, W.-D.; Chung, W.-S. *J. Chin. Chem. Soc. (Taipei, Taiwan)* **2002**, *49*, 77–82.(27) Steele, B. R.; Vrieze, K. *Transition Met. Chem.* **1977**, *2*, 140–144.(28) Abicht, H.-P.; Issleib, K. *J. Organomet. Chem.* **1980**, *185*, 265–275.

intermediate with $[\text{PtCl}_2(\text{SEt}_2)_2]$ is sufficiently hindered by the increased sterics of the ethyl substituents that the dilithium species⁶ persist until they are quenched with water during workup.

The binuclear palladium and platinum organometallic complexes of the C_2N_4 , $[\text{C}_6(\text{CH}_2\text{NR}_2)_4-2,3,5,6]^{2-}$ ligand with a variety of alkylamino substituents were characterized by ^1H NMR and ^{13}C NMR spectroscopy where possible. In general, the neutral palladium and platinum complexes **9–10** have very poor solubility in all solvents tested, and frequently even the ^1H NMR spectra were poorly resolved due to aggregation. Tetrakis(diethylamino) compounds **9a** and **10a**, however, have better solubility than do the tetrakis(dimethylamino) and tetrakis(piperidino) compounds **9b,c** and **10b,c**.

Spectra of the tetrakis(dimethylamino) dinuclear palladium and platinum compounds (**9c** and **10c**) are similar to those reported previously.^{5–6,14–15} The C_2N_4 metal bromides with diethylamino or piperidino substituents (**9a**, **9b**, **10a**, and **10b**) exhibit two characteristic dq and multiplets between 4.19 and 2.62 ppm that are attributable to the diastereotopic protons of the α -carbons of the ethyl or piperidyl groups, respectively. In all four cases, the resonances of the alkyl protons of the alkylamino substituents are at lower field than those of the aryl dibromide precursor (3.45 and 2.62 ppm for **9a** vs 2.52 ppm for **8a**), a downfield shift expected from coordination of the N donors to the newly inserted metals. Similar downfield shifts of the resonances of the α -carbons of alkyl groups of the alkylamino substituents are also shown in ^{13}C NMR (α -carbons of ethyl groups of compound **9a**, 59.2 ppm, and α -carbons of ethyl groups of compound **8a**, 45.8 ppm), consistent with previous reports.^{5–6,14–15}

X-ray molecular structure data of bimetallic compound **10a** (Supporting Information) are similar to previously reported structures.^{5–6,14–15} The crystal structure **11d** shows the oppositely directional coordination sites that make these motifs well suited for use in RPs and supramolecular networks. The weak coordination of between the triflate and palladium is reflected in the inclusion of exogenous water at the labile coordination sites of **11b** when crystals are formed from dichloromethane with 19% hexane and 1% water.^{7c} At question is the extent to which these two coordination sites are appropriately viewed as independent substructures (does coordination at one metal influence coordination at the other?) and whether monomeric analogues are, in general, reasonable model systems for these bimetallic complexes.

Thermodynamics of Pyridine Coordination. The thermodynamics of pyridine coordination are central to many applications of pincer complexes in supramolecular chemistry, and changes in the proton chemical shifts of the bimetallic complex and pyridine ligands upon coordination allow those thermodynamics to be measured by ^1H NMR spectroscopy (Table 1).

Of particular interest in the case at hand is the extent to which there is an influence from the second metal on the thermodynamics of pyridine coordination in these bimetallic complexes. Aryl substrates are known to affect the electronic environment of the pincer metal,²¹ but previous work by

Table 1. Equilibrium Constants, K_{eq} , for Bimetallic Complexes **11–12** or Monometallic Complexes **14** with Pyridine Ligands **13** in DMSO at 25 °C^a

complex	K_{eq} (M^{-1})	complex	K_{eq} (M^{-1})	complex	K_{eq} (M^{-1})
11a·13d	3.3×10	11c·13d	— ^b	12c·13d	1.1×10^4
14a·13d	3.3×10	11b·13d	— ^b	14d·13d	8.0×10^3
11a·13a	1.6×10^3	14b·13d	3.5×10	12a·13d	2.2×10^3
14a·13a	1.3×10^3	11c·13a	— ^b	14c·13d	4.0×10^3
		14b·13a	1.6×10^3		

^a The relevant equilibrium is between pyridine and DMSO coordination and is reported in terms of concentration of functional group. Uncertainties: K_{eq} ($\pm 20\%$). ^b In these cases, the K_{eq} values were not obtained because of overlap in bound and unbound peaks in the ^1H NMR spectrum.

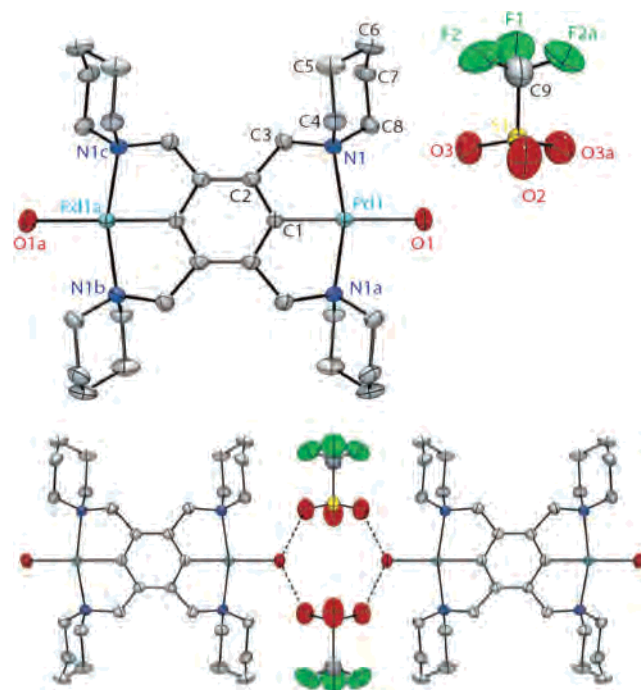


Figure 2. ORTEP drawing of formed **11d**, $[\text{Pd}_2(\text{H}_2\text{O})_2-1,4-\{\text{C}_6(\text{CH}_2\text{N}(\text{CH}_2)_5)_4-2,3,5,6\}]^{+2}(\text{OTf})_2$, from **11b** in 80% dichloromethane with 19% hexane and 1% water. Hydrogen atoms have been omitted for clarity.

Dijkstra et al.,^{1e} Basolo et al.,²⁹ and Yount et al.^{19–20} suggests that the influence of aryl group substituent on coordination kinetics and thermodynamics is, in general, small for this class of metal complexes. To the best of our knowledge, the effect of the second, para metal substituent in 1,4-phenylene-bridged bimetallic complexes has not been reported previously.

We calculated the equilibrium constants for the binding of the pyridine ligands to bimetallic complexes by assuming that the binding sites are independent, so that the equilibrium constants are determined in terms of the concentration of functional groups (the concentration of metal sites is twice that of the bimetallic complex). In DMSO, the “free” metal sites in **11** or **12** exist as the DMSO complex (Figure 3) and small amounts of residual water from solvent or the compounds do not compete with the bulk solvent.²⁰ The equilibrium constant for **11a·13a** (DMSO-*d*₆; 5 mM in **11a** and 10 mM in **13a**) is determined by ^1H NMR to be $1.6 \times 10^3 \text{ M}^{-1}$, within experimental uncertainty of the previously

(29) Basolo, F.; Chatt, J.; Gray, H. B.; Pearson, R. G.; Shaw, B. L. *J. Chem. Soc.* **1961**, 2207–2215.

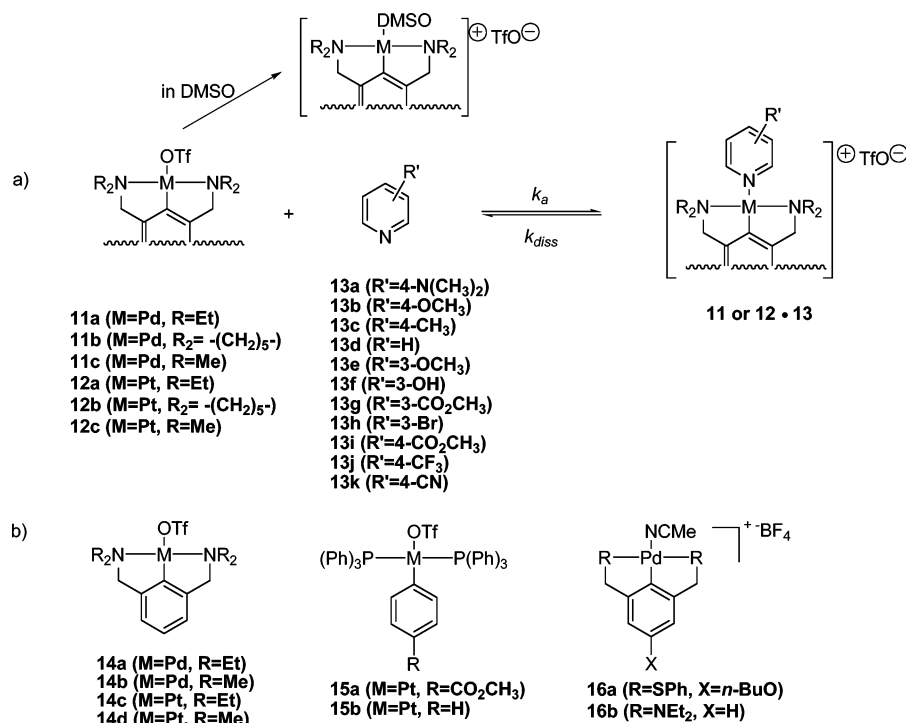


Figure 3. (a) Reversible bimetallic complex–pyridine ligand association. Association and rate constants are expressed in terms of concentration of metal binding sites, which is twice the concentration of the organometallic complex. (b) Monometallic model compound **14**, **15**, and **16**.

Table 2. Equilibrium Constants, K_{eq} , for Ligand Association (25 °C) for Bipalladium Complex **11a**, Biplatinum Complexes **12** or Monoplatinum Complex **15a** with Pyridine Ligands **13** in DMSO-*d*₆^a

complex	K_{eq} (M ⁻¹)	complex	K_{eq} (M ⁻¹)	complex	K_{eq} (M ⁻¹)	complex	K_{eq} (M ⁻¹)
11a · 13a	1.6×10^3	12a · 13a	1.8×10^5	12b · 13b	1.7×10^4	15a · 13a	1.0×10^6
11a · 13b	9.5×10	12a · 13b	1.2×10^4	12b · 13d	1.1×10^4	15a · 13d	3.0×10^4
11a · 13c	3.8×10	12a · 13c	4.6×10^3	12b · 13i	1.4×10^3	15a · 13f	4.0×10^4
11a · 13d	3.3×10	12a · 13d	2.2×10^3	12b · 13j	2.9×10^2	15a · 13g	3.0×10^3
11a · 13e	3.0×10	12a · 13e	2.2×10^3	12c · 13d	1.1×10^4		
		12a · 13h	1.8×10^2	12c · 13e	8.5×10^3		
		12a · 13j	2.1×10^2	12c · 13i	2.3×10^3		
		12a · 13k	1.5×10^2				

^a Uncertainties: K_{eq} ($\pm 20\%$).

reported value of $1.3 \times 10^3 \text{ M}^{-1}$ for monometallic **14a**·**13a**.¹⁹ The result is effectively independent of whether the second metal is coordinated to pyridine (“bound”) or to DMSO (“free”); the measured value is effectively unchanged at 10 mM, at which concentration the majority of bimetallic complexes **11a** have both Pt centers coordinated to **13a**, when compared to that at 2 mM, at which concentration it is more often that **13a** is bound to only one or the two metal centers (1.6×10^3 vs $1.5 \times 10^3 \text{ M}^{-1}$). Similar results are obtained for the weaker complex **11a**·**13d**, where K_{eq} is 3.3×10 (10 mM functional group), 3.2×10 (5 mM functional group), 3.5×10 (2 mM functional groups), and 3.3×10 (1 mM functional group) vs $3.3 \times 10 \text{ M}^{-1}$ for monometallic model complex **14a**·**13d**. Unfortunately, the equilibrium constants of pyridine ligands **13** with bipalladium complex **11b** or **11c** could not be obtained because the chemical shifts for the bound peaks and unbound peaks of complex **11b**·**13** or **11c**·**13** exist in the same position in ¹H NMR spectra. The Pt complex **12a** behaves in a similar manner to Pd complex **11a** (Table 1), although, as expected, pyridine coordination to Pt is stronger than that to Pd ($3.3 \times 10 \text{ M}^{-1}$ for **11a**·**13d**, $2.2 \times 10^3 \text{ M}^{-1}$ for **12a**·**13d**).

In metal-directed assembly, of course, substituted pyridines, rather than the simple ligand **13d**, are ultimately desired. van Manen et al. have previously reported Hammett relationships for the effect of pyridine substituent on complexation to SCS Pd(II) pincer systems.^{22d} For the case of NCN pincer complexes, the effect that substituents on the pyridine ligands have on the equilibrium constant of coordination is seen in the equilibrium constants for the coordination of bipalladium complex **11a** with substituted pyridine ligands **13a**–**13e** (Table 2). As observed in the SCS pincer complexes, K_{eq} for binding increases with the electron-donating character of the substituents (and therefore electron density on the pyridine nitrogen), and a reasonably linear ($R^2 = 0.9445$) free energy relationship between $\log K_{\text{eq}}$ and σ^{30-33} is observed, (Figure 4) where σ is the classic inductive Hammett parameter derived from the ionization of substituted

(30) Aue, D. H.; Webb, H. M.; Bowers, M. T.; Liotta, C. L.; Alexander, C. J.; Hopkins, H. P. *J. Am. Chem. Soc.* **1976**, *98*, 854–856.

(31) (a) Hansch, C.; Leo, A.; Taft, R. W. *Chem. Rev.* **1991**, *91*, 165–195. (b) Voets, R.; Francois, J.-P.; Martin, J. M. L.; Mullens, J.; Yperman, J.; van Poucke, L. C. *J. Comput. Chem.* **1989**, *10*, 449–467.

(32) Maskill, H. *The Physical Basis of Organic Chemistry*; Oxford University Press: Oxford, 1985.

Table 3. Relationship between Substituent Effects on Pyridine Ligands and Pincer Complexes

complex	solvent	ρ	complex	solvent	ρ
11a · 13 (C_2N_4)	DMSO- d_6	-1.9 ± 0.4	15b · 13 (PCP)	DMSO- d_6	-1.7 ± 0.3
12a · 13 (C_2N_4)	DMSO- d_6	-2.1 ± 0.4	16a · 13 (SCS)	CDCl ₃	-0.8 ± 0.2^a
15a · 13 (PCP)	DMSO- d_6	-1.9 ± 0.4	16b · 13 (NCN)	CDCl ₃	-1.3 ± 0.2

^a Data taken from ref 22d.

benzoic acids.³⁴ The ρ value, -1.9 , is significantly lower than that determined for aqueous pK_a 's ($\rho = -5.9$)³⁰ and gas phase ($\rho = -13.6$)³¹ proton affinities of substituted pyridines. The classical view is that electron-donating pyridine substituents influence the coordination ability in two offsetting manners:²² by increasing the σ -donating ability of the ligand and simultaneously decreasing its π -acceptor ability. It is also possible that π -donating effects could play a role. While the nature of the bonding is undoubtedly more complex than simple σ donation, however, the free energy relationship in Figure 4 is sufficiently linear as to be useful for guiding the design of systems with appropriate free energies of association for a given endpoint. Unlike a previous example of Co–picoline coordination reported by Nelson,³⁵ no evidence for dramatic meta substituent effects is observed here (3-methoxypyridine, empty diamond, Figure 4).

When the metal center is changed from Pd(II) to Pt(II), a similar pattern is observed (Table 2 and Figure 5). Decreasing the electron-donating ability of the substituents, as expected, leads to a decrease in K_{eq} for the association of complex **12a** with pyridine ligands **13a–13e**, **13h**, and **13j–13k**. Interestingly, the magnitude of the dependence ($\rho = -2.1$) is very similar to that observed with complex **11a**, although

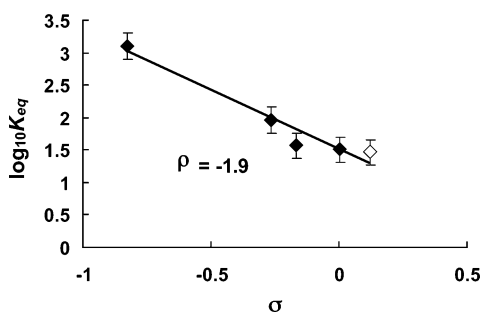


Figure 4. Linear free energy relationship of $\log K_{eq}$ vs σ values for bipalladium complex **11a** with pyridine ligands **13a–13e** (filled diamonds = 4-substituted pyridines, empty diamond = 3-substituted pyridines).

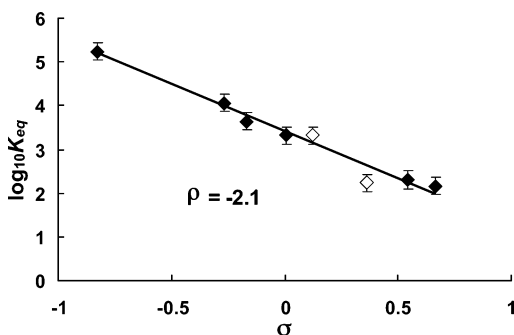


Figure 5. Linear free energy relationship of $\log K_{eq}$ vs σ values for biplatinum complex **12a** with pyridine ligands **13a–13e**, **13h**, and **13j–13k** (filled diamonds = 4-substituted pyridines, empty diamonds = 3-substituted pyridines).

Table 4. Ligand-Exchange Kinetics, k_d , for Bimetallic Complexes **12a** or Monometallic Complexes **14** with Pyridine Ligands **13** in DMSO- d_6 at 25 °C

complex	k_d (s^{-1})	complex	k_d (s^{-1})
14a · 13a	100 ^a	14c · 13d	0.0006 ^c
14a · 13d	17 ^b	14d · 13d	0.026 ^c
14b · 13a	1 ^a	12a · 13d	0.0005
14b · 13d	1450 ^b		

^a Data taken from ref 19. ^b Data taken from ref 20b. ^c Data taken from ref 20a

the absolute association constants of common pyridine ligands are a factor of ~ 100 greater. Because the operative equilibrium is that between pyridine and DMSO coordination, these results are consistent with the common view that DMSO (which typically coordinates to Pd(II) and Pt(II) through sulfur³⁶) does not behave simply as a weaker version of pyridine in the continuum of binding strengths.³⁷ The equilibrium constants, K_{eq} , for the associations of complex **12b** or **12c** with pyridine ligands are summarized in Table 2.

It is interesting to compare the thermochemical features of coordination in the pincer complexes to the bis(triphenylphosphine) aryl–Pt(II) motif **15a**,³⁸ whose use is well-established within metal-directed supramolecular assembly. Replacing the cis pincer alkylamino substituents with the triphenylphosphines favors pyridine binding vs DMSO by an additional factor of 10 (Table 2, Table 3), perhaps due to the additional π -accepting character of the phosphines, but again discrimination within the family of substituted pyridines is effectively unchanged ($\rho = -1.9$). Effectively equivalent absolute and relative equilibrium constants are observed for the related metal complex **15b** ($\rho = -1.7$, data not shown). The relative binding of pyridines vs DMSO in aryl Pd(II) and Pt(II) complexes, therefore, appear to be generally unaffected by substitution on the trans organometallic aryl group. The competition between pyridines and DMSO is significantly influenced, however, by changes in either the metal or the cis ligands. Previously, van Manen et al. showed that the effect of pyridine substituent on complexation to SCS–Pd(II) pincer systems **16a**.^{22d} When their

(33) Johnson, C. D. *The Hammett Equation*; Cambridge University Press: Cambridge, 1973.

(34) Previous work by van Manen et al.^{22d} on SCS–pincer complexes interpreted the substituent effect in terms of the Brown–Okamoto σ^+ substituent constant. The linear free energy relationships for σ^+ and σ give comparable correlation coefficients for the series examined here, and we use σ as the basis for discussion. None of the conclusions of this work are contingent on the choice of σ vs σ^+ .

(35) Nelson, S. M.; Shepherd, T. M. *Inorg. Chem.* **1965**, *4*, 813–817.

(36) Calligaris, M. *Coord. Chem. Rev.* **2004**, *248*, 351–375.

(37) (a) Pribula, A. J.; Drago, R. S. *J. Am. Chem. Soc.* **1976**, *98*, 2784–2788. (b) Kroeger, M. K.; Drago, R. S. *J. Am. Chem. Soc.* **1981**, *103*, 3250–3262.

(38) Manna, J.; Whiteford, J. A.; Stang, P. J.; Muddiman, D. C.; Smith, R. D. *J. Am. Chem. Soc.* **1996**, *118*, 8731–8732.

data is plotted against σ ,^{22d} a ρ value of -0.8 ± 0.2 is obtained. The van Manen study differs from the current experiments in several respects: the pincer ligands (SPh vs NEt₂), the counterion (BF₄⁻ vs TfO⁻), and the solvent (chloroform + stoichiometric CH₃CN vs DMSO). To address only the effect of pincer ligand, we synthesized NCN–pincer complex **16b**¹⁹ and obtained its ρ value for pyridine coordination in CDCl₃. In this case, the ρ value is -1.3 ± 0.2 , slightly reduced from that of **11a**·**13** ($\rho = -1.9 \pm 0.4$) in DMSO. The measured ρ values are sensitive to the solvent and/or counterion, even though these species are not formally involved in competition between different pyridines. Their results suggest that differential solvation of pyridines and their pincer complex is sensitive to pyridine substituent, and that affects equivalent as much as choice of metal or amine vs phosphine.³⁹

Ligand-Exchange Kinetics. In addition to the thermodynamics of coordination, the rate of ligand dissociation is often an important consideration in dynamic, metal-directed assemblies. The rate of pyridine exchange was measured by monitoring the replacement of complexed pyridine **13d** with its deuterated equivalent, **13d-d₅**. Pyridine displacement from these pincer complexes in DMSO occurs through a solvent-assisted process,^{20b} and the effectively first-order rate constant obtained from early time points (<20% substitution) of pyridine exchange in the bimetallic complex **12a**·**13d** ($0.0005 \pm 0.0001 \text{ s}^{-1}$) is within experimental error of that reported previously²⁰ for monomeric model complex **14b**·**13d** ($0.0006 \pm 0.0001 \text{ s}^{-1}$). The agreement in the two values is consistent with a minimal substituent effect in substituted trans-aryl Pd(II) and Pt(II) complexes^{19,29} and further supports the meaningful use of model complexes such as **14b** to describe kinetic, as well as thermodynamic, behavior in the bimetallic complexes.

Conclusion

The association constants of pyridine coordination to 1,4-phenylene-bridged bipalladium and biplatinum pincer complexes in DMSO have been determined by ¹H NMR spectroscopy. The two metal sites act as independent coordination sites for pyridine, and the thermodynamics of pyridine coordination are effectively unchanged from those of monometallic model complexes. The affinity for pyridine vs DMSO increases as the metal changes from Pd to Pt or as the pincer alkylamino substituents are replaced by triphenylphosphines. For each of the organometallic compounds, pyridine coordination increases with electron-donating substituents at the para position, although the effect of those substituents likely reflects a combination of increased σ -donating strength and decreased π -accepting

ability. Hammett linear free energy relationships for coordination of substituted pyridines are nearly identical for Pd vs Pt and pincer amine vs triphenylphosphine cis ligands, and the competition between pyridines is as sensitive to solvent (DMSO-*d*₆ vs CDCl₃) as it is to any of these variations in pincer structure. As with the thermodynamics, no significant change in the kinetics of ligand exchange is observed from the monometallic to bimetallic complex.

These results have several implications in the broader context of reversible polymers and supramolecular networks. First, the kinetic and thermodynamic independence of the coordination events simplifies the interpretation of their behavior in those materials, where the relative population of, and rates of transition between, a state of two vs one coordinated ligand determine molecular weights and mechanical properties. Second, the similarity in the thermodynamic and kinetic parameters with those measured on model, monometallic systems corroborates the use of those model systems as a reasonable anchor for determining molecule-to-material relationships. Finally, the quantitative structure–activity relationships establish a baseline by which the thermodynamics of coordination can be readily engineered for particular outcomes.

Experimental

Materials and Methods. DMSO (Acros), dichloromethane (Acros), and pyridine ligands **13a**–**13k** (Aldrich) were used as received. Solvents were dried and stored under nitrogen. Deuterated solvents, DMSO-*d*₆ and CDCl₃, were purchased from CIL (Cambridge Isotope Laboratories, Inc.) ¹H NMR spectra were acquired using a Varian 400 MHz spectrometer. ¹³C NMR spectra were acquired at 100 MHz. Mass spectra were acquired by Georgy Dubay at Duke University. Elemental analysis data were obtained from M-H-W laboratories, Phoenix, AZ.

Equilibrium Constants. The equilibrium constants, K_{eq} , of metal–ligand coordination were determined by ¹H NMR spectroscopy. For example, pincer complex **11a** (5 mM) and pyridine **13d** (10 mM) were dissolved in DMSO-*d*₆, introduced into an NMR tube, and shaken. After 10 min, or long enough time to ensure equilibration, NMR spectra were recorded. Separate ¹H NMR peaks were observed for the methylene protons of bound and free **11a** (3.86 ppm for free **11a**, 3.99 ppm for **11a** bound to pyridine) and the ortho protons of bound and free **13d** (8.58 ppm for free pyridine **13d**, 8.80 ppm for pyridine bound to **11a**). The integrations of the free and bound species were used to calculate the equilibrium constant of the complex, determined in terms of concentration of functional groups (concentration of total metal sites is twice that of the bimetallic complexes).

Exchange Kinetics. NMR spectra were acquired using a Varian 400 MHz spectrometer as follows. A DMSO-*d*₆ solution of metal compound (**12a**, 5 mM) and pyridine ligand (**13d**, 10 mM) was equilibrated, and a ¹H NMR spectrum recorded. Deuterated pyridine (**13d-d₅**) was added to the solution to give a final concentration of 20 mM in **13d-d₅**. The solution was inverted several times in the NMR tube to mix the reactants, and the sample was returned to the spectrometer. ¹H NMR spectra were taken every 15 min for 4 h. Spectra were then analyzed to determine the amount of bound and free species (ortho aryl protons, bound at 8.85–8.84 ppm/free at 8.56–8.55 ppm) of **13d**.

X-ray Structure Determination of Compound 10a and the Hydrate of 11d. Diffraction data were collected using a Bruker

(39) Differential solvation has been implicated in ligand-exchange kinetics, for example, nucleophilic substitution reaction of platinum^{39a–c} and palladium complex.^{39d} (a) Romeo, R.; Tobe, M. L.; Trozzi, M. *Inorg. Chim. Acta* **1974**, *11*, 231–236. (b) Pitteri, B.; Cattalini, L.; Chessa, G.; Marangoni, G.; Stevanato, N.; Tobe, M. L. *J. Chem. Soc., Dalton Trans.* **1991**, 3049–3054. (c) Alibrandi, G.; Romeo, R.; Scolaro, L. M.; Tobe, M. L. *Inorg. Chem.* **1992**, *31*, 5061–5066. (d) Canovese, L.; Cattalini, L.; Uguagliati, P.; Tobe, M. L. *J. Chem. Soc., Dalton Trans.* **1990**, 867–872.

Smart Diffractometer (**10a**) and Bruker Kappa Diffractometer (**11d**) equipped with an Apex II detector at room temperature. Data were collected at 10 s per frame for the whole hemisphere. The data were processed with Apex II software and the structure was solved and refined using Apex II software (see Supporting Information).

Synthesis. Compounds **6**,²⁵ **8c**,¹⁴ **14**,^{19–20} **15a**,^{20b} **15b**,^{19–20} **16b**,^{19,22d} [PtCl₂(SEt₂)₂]²⁸ and [Pt(*p*-tolyl)₂(SEt₂)₂]²⁷ were synthesized according to literature procedure.

1,4-Dibromo- $\{2,3,5,6\}$ -tetrakis(bromomethyl)benzene, 1,4-C₆Br₂(CH₂Br)_{4-2,3,5,6} (7). Compound **7**^{26a} was generated by a previously published process^{26b} used to make the 1,2,4,5-tetrakis-(bromomethyl)benzene. *N*-Bromosuccinimide (12.816 g, 0.072 mol) was added to a stirred solution of **6** (2.920 g, 0.01 mol) in CHCl₃ (150 mL) at room temperature. The reaction mixture was heated to reflux and stirred for 5 h, at which time the product had precipitated. The reaction mixture was allowed to cool to room temperature, and the product was filtered and washed with cold dichloromethane (5 × 100 mL). The white solid was dried under vacuum. Yield 75% (4.560 g). ¹H NMR (CDCl₃) δ 4.84 (s, 8H, PhCH₂). ¹³C NMR (CDCl₃) δ 153.1, 128.4, 30.7. HRMS (FAB) *m/z* 607.5659 (M⁺, C₁₀H₈Br₆, calcd 607.5665). The resulting white solid was used in the subsequent amination without further purification.

1,4-Dibromo- $\{2,3,5,6\}$ -tetrakis{(diethylamino)methyl}benzene, 1,4-C₆Br₂(CH₂NEt₂)_{4-2,3,5,6} (8a). Compound **8a** was generated using the procedure reported previously for **8c**.¹⁴ Compound **7** (6.080 g, 0.01 mol) was added to a stirred solution of diethylamine (21.942 g, 0.30 mol) in THF (60 mL) at –10 °C. The reaction mixture was allowed to warm to room temperature over a period of 1 h and then heated to 55 °C for 5 min. The reaction mixture was allowed to cool to room temperature, and all volatiles were removed under vacuum to leave a white solid residue. This residue was suspended in aqueous NaOH (100 mL, 2 M), and with vigorous stirring of the mixture, Et₂O (300 mL) was added. Stirring was stopped, from the resulting two-layer system the organic layer was collected, and the water layer extracted with Et₂O (200 mL). The combined organic layer and extracts were washed with saturated aqueous NaCl (100 mL) and dried with MgSO₄. The solution was filtered and the volume reduced under vacuum. The resulting white solid was dried under vacuum. Yield 91% (5.246 g). ¹H NMR (CDCl₃) δ 4.11 (s, 8H, PhCH₂), 2.52 (q, *J* = 7.1 Hz, 16H, NCH₂), 0.94 (t, *J* = 7.1 Hz, 24H, CH₃). ¹³C NMR (CDCl₃) δ 140.1, 132.6, 55.7, 45.8, 11.8. HRMS (FAB) *m/z* 577.2308 ([M + H]⁺, C₂₆H₄₉N₄Br₂, calcd 577.2304). The product was carried on to subsequent metalation products, **9a** and **10a**, without further purification.

1,4-Dibromo- $\{2,3,5,6\}$ -tetrakis{methylpiperidyl}benzene, 1,4-C₆Br₂[CH₂N(CH₂)₅]_{4-2,3,5,6} (8b). Compound **8b** was synthesized according to the procedure for **8a**. The resulting white solid was dried under vacuum. Yield 92% (5.746 g). ¹H NMR (CDCl₃) δ 4.07 (s, 8H, PhCH₂), 2.40 (s, 16H, NCH₂), 1.46–1.39 (m, 24H, CH₂). ¹³C NMR (CDCl₃) δ 139.3, 132.8, 59.6, 54.7, 26.4, 24.7. HRMS (FAB) *m/z* 625.2305 ([M + H]⁺, C₃₀H₄₉N₄Br₂, calcd 625.2295). The product was used in the synthesis of the metallated products, **9b** and **10b**, without further purification.

$\{2,3,5,6\}$ -Tetrakis{(diethylamino)methyl}phenylene-1,4-bis{bromopalladium(II)}, [(PdBr)₂-1,4-{C₆(CH₂NEt₂)_{4-2,3,5,6}}] (9a). Compound **8a** (1.441 g, 2.50 mmol) was dissolved in dry toluene (50 mL). Pd₂(dba)₃ (2.562 g, 2.80 mmol) was added, and the solution was stirred and heated to 90 °C for 36 h. The solution was then filtered through celite and washed with toluene until the yellow color on celite was washed through. The celite was then washed with hot chloroform (1 L) into a clean flask. The chloroform

solution was reduced to volume under vacuum, and the product (yellow solid) was purified using flash chromatography (SiO₂, CHCl₃/CH₃OH = 97:3). The resulting yellow solid was dried under vacuum. Yield 94% (1.855 g). ¹H NMR (CDCl₃) δ 3.73 (s, 8H, PhCH₂), 3.45(dq, *J* = 12.0 Hz, 7.0 Hz, 8H, NCH₂), 2.62 (dq, *J* = 12.0 Hz, 7.0 Hz, 8H, NCH₂), 1.57 (t, *J* = 7.0 Hz, 24H, CH₃). ¹³C NMR (CD₂Cl₂) δ 151.0, 138.3, 65.7, 59.2, 14.5. Anal. Calcd for C₂₆H₄₈Br₂N₄Pt₂: C, 39.56; H, 6.13; N, 7.10. Found; C, 39.73; H, 6.11; N, 7.11. HRMS (FAB) *m/z* 706.1153 ([M – Br]⁺, C₂₆H₄₈N₄BrPd₂, calcd 706.1148).

$\{2,3,5,6\}$ -Tetrakis(methylpiperidyl)phenylene-1,4-bis{bromopalladium(II)}, [(PdBr)₂-1,4-{C₆(CH₂NEt₂)_{4-2,3,5,6}}] [(PdBr)₂-1,4-{C₆(CH₂N(CH₂)₅)_{4-2,3,5,6}}] (9b). Compound **9b** was synthesized according to the procedure for **9a**. The reaction mixture was filtered through filter paper and then washed with toluene (3 × 20 mL). The solid on the filter paper was washed with cold diethyl ether (5 × 20 mL) and then washed twice with a cold solvent mixture of diethylether (15 mL) and dichloromethane (5 mL). The resulting yellow solid was dried under vacuum. Yield 81% (1.696 g). ¹H NMR (CDCl₃) δ 4.19–3.95 (m, 8H, NCH₂), 4.04 (s, 8H, PhCH₂), 3.27 (br s, 8H, NCH₂), 1.72–1.42 (m, 24H, CH₂). ¹³C NMR and mass spectra could not be obtained due to the poor solubility of compound **9b**, but the structure was confirmed from its subsequent conversion to **11b**. The product was converted directly into the triflated product, **11b**, without further purification.

$\{2,3,5,6\}$ -Tetrakis{(dimethylamino)methyl}phenylene-1,4-bis{bromopalladium(II)}, [(PdBr)₂-1,4-{C₆(CH₂NMe₂)_{4-2,3,5,6}}] (9c). Compound **9c** was synthesized according to the procedure for **9b**. The resulting white solid was dried under vacuum. Yield 83% (1.405 g). ¹H NMR (CDCl₃) δ 3.79 (s, 8H, PhCH₂), 2.92 (s, 24H, NCH₃). ¹³C NMR and mass spectra could not be obtained due to the poor solubility of compound **9c**, but the structure was confirmed from its subsequent conversion to **11c**. The product was converted directly into the triflated product, **11c**, without further purification.

$\{2,3,5,6\}$ -Tetrakis{(diethylamino)methyl}phenylene-1,4-bis{bromoplatinum(II)}, [(PtBr)₂-1,4-{C₆(CH₂NEt₂)_{4-2,3,5,6}}] (10a). Compound **8a** (2.000 g, 3.47 mmol) was dissolved in dry toluene (75 mL). [Pt(*p*-tolyl)₂(SEt₂)₂] (4.541 g, 4.82 mmol) was added, and the solution was stirred and heated to 90 °C for 36 h. The solution was then filtered through celite and washed with toluene until the yellow color on celite was washed through. The celite was then washed with dichloromethane (1 L) into a clean flask, and the volume of the dichloromethane solution was reduced under vacuum. The product was purified using flash chromatography (SiO₂, CHCl₃/CH₃OH = 97:3). The resulting yellow solid was dried under vacuum. Yield 72% (2.415 g). ¹H NMR (CDCl₃) δ 3.81 (s, 8H, ³J_{Pt–H} = 32.8 Hz, PhCH₂), 3.51 (dq, *J* = 12.1 Hz, 7.1 Hz, 8H, NCH₂), 2.84 (dq, *J* = 12.1 Hz, 7.1 Hz, 8H, NCH₂), 1.49 (t, *J* = 7.1 Hz, 24H, CH₃). ¹³C NMR (CDCl₃) δ 133.2, 68.7, 60.6, 13.7. Anal. Calcd for C₂₆H₄₈Br₂N₄Pt₂: C, 32.31; H, 5.01; N, 5.80. Found; C, 32.26; H, 4.93; N, 5.74. HRMS (FAB) *m/z* 884.2305 ([M – Br]⁺, C₂₆H₄₈N₄BrPt₂, calcd 884.2337). X-ray molecular structure data of bimetallic complex **10a** are available in the Supporting Information.

$\{2,3,5,6\}$ -Tetrakis(methylpiperidyl)phenylene-1,4-bis{bromoplatinum(II)}, [(PtBr)₂-1,4-{C₆(CH₂N(CH₂)₅)_{4-2,3,5,6}}] (10b). Compound **10b** was synthesized according to the procedure for **10a**. The reaction mixture was filtered through filter paper and then washed with toluene (3 × 20 mL). The solid was washed with a cold diethylether (5 × 20 mL) and then washed twice with a cold solvent mixture of diethylether (15 mL) and dichloromethane (5 mL). The resulting pale yellow solid was dried under vacuum. Yield 79% (2.782 g). ¹H NMR (CDCl₃) δ 4.13–3.97 (m, 8H, NCH₂,

$^3J_{\text{Pt-H}}$ were not observed, a fact we attribute to the poor solubility of the compound), 4.07 (s, 8H, PhCH₂), 3.26–3.23 (m, 8H, NCH₂), 1.74–1.36 (m, 24H, CH₂). ¹³C NMR and mass spectra could not be obtained due to the poor solubility of compound **10b**, but the structure was confirmed from its subsequent conversion to **12b**. The product was converted directly into the triflated product, **12b**, without further purification.

[2,3,5,6-Tetrakis{(dimethylamino)methyl}phenylene-1,4-bis-bromoplatinum(II)], [(PtBr)₂-1,4-{C₆(CH₂NMe₂)₄-2,3,5,6}] (**10c**). Compound **10c** was synthesized according to the procedure for **10b**. The resulting white solid was dried under vacuum. Yield 81% (2.401 g). ¹H NMR (CDCl₃) δ 3.85 (s, 8H, PhCH₂, $^3J_{\text{Pt-H}}$ not observed due to very poor S/N ratio), 3.07 (s, 24H, NCH₃, $^3J_{\text{Pt-H}}$ not observed due to very poor S/N ratio). ¹³C NMR and mass spectra could not be obtained due to the poor solubility of compound **10b**, but the structure was confirmed from its subsequent conversion to **12c**. The product was converted directly into the triflated product, **12c**, without further purification.

[2,3,5,6-Tetrakis{(diethylamino)methyl}phenylene-1,4-bis(palladiumtrifluoromethanesulfonate)], [(PdOTf)₂-1,4-{C₆(CH₂NEt₂)₄-2,3,5,6}] (**11a**). Compound **9a** (0.553 g, 0.70 mmol) was dissolved in dichloromethane (75 mL), and the reaction flask was wrapped by aluminum foil. AgOTf (0.389 g, 1.50 mmol) was added to the reaction mixture at 0 °C. The solution was stirred for 24 h at room temperature and, after the aluminum foil was removed, stirred for an additional 4 h. The reaction mixture was filtered, the solid washed with dichloromethane (3 × 100 mL), and the solvent was evaporated. The resulting yellow solid was dried under vacuum. Yield 96% (0.623 g). ¹H NMR (CDCl₃) δ 3.72 (s, 8H, PhCH₂), 3.22 (dq, *J* = 12.6 Hz, 7.1 Hz, 8H, NCH₂), 2.65 (dq, *J* = 12.6 Hz, 7.1 Hz, 8H, NCH₂), 1.57 (t, *J* = 7.1 Hz, 24H, CH₃). ¹H NMR (CD₃OD) δ 3.90 (s, 8H, PhCH₂), 3.00 (dq, *J* = 12.8 Hz, 7.0 Hz, 8H, NCH₂), 2.74 (dq, *J* = 12.8 Hz, 7.0 Hz, 8H, NCH₂), 1.54 (t, *J* = 7.0 Hz, 24H, CH₃). ¹³C NMR (CDCl₃) δ 144.9, 137.8, 64.6, 57.4, 14.0. ¹³C NMR (CD₃OD) δ 146.3, 139.4, 65.4, 58.4, 14.4. MS (FAB) *m/z* 928 ([M + 1]⁺, 3), 926 ([M - 1]⁺, 3), 779 (100), 777 (80), 630 (6), 524 (6). HRMS (FAB) *m/z* 777.1405 ([M - CF₃SO₃]⁺, C₂₇H₄₈O₃N₄F₆SPd₂, calcd 777.1411). Anal. Calcd for C₂₈H₄₈O₆N₄F₆S₂Pd₂: C, 36.25; H, 5.22; N, 6.04. Found; C, 36.36; H, 5.28; N, 5.95. Complex **11a** was used immediately in the thermodynamic study after isolation.

[2,3,5,6-Tetrakis(methylpiperidyl)phenylene-1,4-bis(palladiumtrifluoromethanesulfonate)], [(PdOTf)₂-1,4-{C₆(CH₂N(-CH₂)₅)₄-2,3,5,6}] (**11b**). Compound **11b** was synthesized according to the procedure for **11a**. The reaction mixture was filtered, the solid washed with dichloromethane (90 mL) and methanol (10 mL), and the solvent was evaporated. The resulting white solid was dried under vacuum. Yield 94% (0.642 g). ¹H NMR (CDCl₃) δ 4.07 (br s, 8H, PhCH₂), 3.78–3.72 (m, 8H, NCH₂), 3.23–3.19 (m, 8H, NCH₂), 1.74–1.46 (m, 24H, CH₂). ¹H NMR (CD₃OD) δ 4.24 (s, 8H, PhCH₂), 3.36–3.29 (m, 8H, NCH₂), 3.19–3.16 (m, 8H, NCH₂), 1.92–1.86 (m, 8H, CH₂), 1.70–1.67 (m, 4H, CH₂), 1.58–1.45 (m, 12H, CH₂). ¹³C NMR (CD₃OD) δ 150.5, 137.4, 68.0, 62.3, 24.4, 22.6. MS (FAB) *m/z* 976 ([M + 1]⁺, 1), 974 ([M - 1]⁺, 1), 827 (100), 825 (89), 768 (8), 572 (22). HRMS (FAB) *m/z* 825.1468 ([M - CF₃SO₃]⁺, C₃₁H₄₈F₃N₄O₃Pd₂S, calcd 825.1471). X-ray molecular structure data of formed **11d** from **11b** are available in the Supporting Information. Anal. Calcd for C₃₂H₄₈F₆N₄O₆-Pd₂S₂: C, 39.39; H, 4.96; N, 5.74. Found; C, 39.02; H, 4.82; N, 5.63. Complex **11b** was used immediately in the thermodynamic study after isolation.

[2,3,5,6-Tetrakis{(dimethylamino)methyl}phenylene-1,4-bis(palladiumtrifluoromethanesulfonate)], [(PdOTf)₂-1,4-{C₆(CH₂-

NMe₂)₄-2,3,5,6}] (**11c**). Compound **11c** was synthesized according to the procedure for **11b**. The resulting white solid was dried under vacuum. Yield 97% (0.554 g). ¹H NMR (CD₃OD) δ 3.86 (s, 8H, PhCH₂), 2.74 (s, 24H, NCH₃). ¹³C NMR (CD₃OD) δ 148.8, 138.9, 72.6, 52.6. MS (FAB) *m/z* 816 ([M + 1]⁺, 3), 814 ([M - 1]⁺, 1), 667 (100), 665 (90), 613 (24), 518 (21). HRMS (FAB) *m/z* 665.0221 ([M - CF₃SO₃]⁺, C₁₉H₃₂F₃N₄O₃Pd₂S, calcd 665.0216). Anal. Calcd for C₂₀H₃₂F₆N₄O₆Pd₂S₂: C, 29.46; H, 3.96; N, 6.87. Found; C, 29.36; H, 4.04; N, 6.73. Complex **11c** was used immediately in the thermodynamic study after isolation.

[2,3,5,6-Tetrakis{(diethylamino)methyl}phenylene-1,4-bis-(platinumtrifluoromethanesulfonate)], [(PtOTf)₂-1,4-{C₆(CH₂NEt₂)₄-2,3,5,6}] (**12a**). Compound **12a** was synthesized according to the procedure for **11a**. The resulting yellow solid was dried under vacuum. Yield 95% (0.735 g). ¹H NMR (CD₃OD) δ 3.95 (s, 8H, $^3J_{\text{Pt-H}}$ = 46.4 Hz, PhCH₂), 3.06 (dq, *J* = 12.5 Hz, 7.1 Hz, 8H, NCH₂), 2.90 (dq, *J* = 12.5 Hz, 7.1 Hz, 8H, NCH₂), 1.42 (t, *J* = 7.1 Hz, 24H, CH₃). ¹³C NMR (CD₃OD) δ 149.7, 137.3, 68.4, 60.4, 13.8. MS (FAB) *m/z* 1104 (M⁺, 3), 955 (100), 847 (17), 806 (8), 775 (8). HRMS (FAB) *m/z* 954.2678 ([M - CF₃SO₃]⁺, C₂₇H₄₈F₃-N₄O₃Pt₂S, calcd 954.2674). Anal. Calcd for C₂₈H₄₈F₆N₄O₆Pt₂S: C, 30.43; H, 4.38; N, 5.07. Found; C, 30.36; H, 4.39; N, 4.99. Complex **12a** was used immediately in the thermodynamic study after isolation.

[2,3,5,6-Tetrakis(methylpiperidyl)phenylene-1,4-bis(platinumtrifluoromethanesulfonate)], [(PtOTf)₂-1,4-{C₆(CH₂N(-CH₂)₅)₄-2,3,5,6}] (**12b**). Compound **12b** was synthesized according to the procedure for **11b**. The resulting yellow solid was dried under vacuum. Yield 96% (0.775 g). ¹H NMR (CD₃OD) δ 4.12 (s, 8H, $^3J_{\text{Pt-H}}$ = 40.8 Hz, PhCH₂), 3.31–3.23 (m, 8H, NCH₂), 3.10–3.07 (m, 8H, NCH₂), 1.87–1.81 (m, 8H, CH₂), 1.63–1.53 (m, 4H, CH₂), 1.50–1.46 (m, 12H, CH₂). ¹³C NMR (CD₃OD) δ 149.3, 139.0, 65.9, 60.4, 24.6, 22.3. MS (FAB) *m/z* 1153 (M⁺, 4), 1103 (100), 854 (11), 740 (16). HRMS (FAB) *m/z* 1003.2659 ([M - CF₃SO₃]⁺, C₃₁H₄₈F₃N₄O₃Pt₂S, calcd 1003.2656). Anal. Calcd for C₃₂H₄₈F₆N₄O₆-Pt₂S₂: C, 33.33; H, 4.20; N, 4.86. Found; C, 33.28; H, 4.07; N, 4.60. Complex **12b** was used immediately in the thermodynamic study after isolation.

[2,3,5,6-Tetrakis{(dimethylamino)methyl}phenylene-1,4-bis-(platinumtrifluoromethanesulfonate)], [(PtOTf)₂-1,4-{C₆(CH₂NMe₂)₄-2,3,5,6}] (**12c**). Compound **12c** was synthesized according to the procedure for **11b**. The resulting yellow solid was dried under vacuum. Yield 97% (0.554 g). ¹H NMR (CD₃OD) δ 3.86 (s, 8H, $^3J_{\text{Pt-H}}$ = 44.4 Hz, PhCH₂), 2.74 (s, 24H, $^3J_{\text{Pt-H}}$ = 32.0 Hz, NCH₃). ¹³C NMR (CD₃OD) δ 138.9, 137.3, 75.1, 54.2. MS (FAB) *m/z* 992 (M⁺, 1), 843 (100), 734 (19), 694 (26), 613 (55). HRMS (FAB) *m/z* 841.1390 ([M - CF₃SO₃]⁺, C₁₉H₃₂O₃N₄F₃Pt₂S, calcd 841.1401). Anal. Calcd for C₂₀H₃₂O₆N₄F₆Pt₂S₂: C, 24.20; H, 3.25; N, 5.64. Found; C, 24.40; H, 3.50; N, 5.39. Complex **12c** was used immediately in the thermodynamic study after isolation.

Acknowledgment. We thank NSF and NIH for funding and acknowledge Burroughs-Wellcome Fellowships to D.M.L. and W.C.Y. We thank R. Widenhoefer and A. Crumbliss for helpful discussions and D. Pham, J. Jiang, and K. Franz for solving the crystal structures.

Supporting Information Available: X-ray molecular structure data of bimetallic complexes **10a** and **11d** and ¹H NMR spectra of complexes **11**–**12** in CD₃OD. This material is available free of charge via the Internet at <http://pubs.acs.org>.

IC061188B